

Quick Assessment of the Thermal Decomposition Behavior of Lignocellulosic Biomass by Near Infrared Spectroscopy and Its Statistical Analysis

Seung-Hwan Lee,^{1,2} Hyun-Woo Cho,³ Nicole Labbé,² Myong K. Jeong⁴

¹Biomass Technology Research Center, National Institute of Advanced Industrial Science and Technology, Suehiro 2-2-2, Hiro, Kure, Hiroshima, Japan

²Tennessee Forest Products Center, University of Tennessee, 2506 Jacob Drive, Knoxville, Tennessee 37996-4570

³Department of Industrial and Information Engineering, University of Tennessee, East Stadium Hall, Knoxville, Tennessee 37996

⁴Department of Industrial and Systems Engineering & RUTCOR, Rutgers, the State University of New Jersey, 640 Bartholomew Road, Piscataway, New Jersey 08854

Received 25 February 2008; accepted 16 January 2009

DOI 10.1002/app.30119

Published online 7 August 2009 in Wiley InterScience (www.interscience.wiley.com).

ABSTRACT: The application of near infrared (NIR) spectroscopy for the prediction of the thermal decomposition behavior of lignocellulosic biomass (three types of woody biomass and three types of herbaceous biomass) was successfully performed along with statistical analysis. The thermal degradation behaviors of the woody and herbaceous biomass were different because of their different chemical compositions. Herbaceous biomass was degraded at lower temperature than woody biomass. The weight-loss profiles as a function of temperature were obtained by thermogravimetric analysis (TGA) at a heating rate of 25°C/min under nitrogen gas. The weight-loss percentage at 10 temperatures in the range 150–600°C was predicted

by a wavelet partial least squares (PLS) model, which showed significantly better predictive performance than the ordinary PLS model. The results show that the data predicted by the wavelet PLS model was well fitted to the original data by TGA, in which the root-mean-square error in prediction values less than 5.5 suggested that NIR spectroscopy was applicable for rapid analysis to characterize the thermal decomposition behavior of lignocellulosic biomass for energy production. © 2009 Wiley Periodicals, Inc. *J Appl Polym Sci* 114:3229–3234, 2009

Key words: biomaterials; degradation; NIR; thermal properties; thermogravimetric analysis (TGA)

INTRODUCTION

Lignocellulosic biomass has become a promising raw feedstock for bioenergy and other biobased products because of its abundance, renewability, and other environmental benefits. Various methods have been used to convert lignocellulosic biomass into bioenergy. These include microbial and enzymatic processes to produce ethanol^{1–5} and thermochemical processes (e.g., pyrolysis, gasification, direct liquefaction) to produce synthesis gas (so-called Syngas) consisting primarily of carbon monoxide, carbon dioxide, and hydrogen or pyrolysis oils (bio-oil).^{6,7}

In thermochemical processes, especially pyrolysis and gasification, the thermal decomposition behavior is crucial to the understanding of the reaction mechanism and the characteristics of the end products.

As is well known, biomass thermal decomposition proceeds through a series of complex reactions that are dependent on chemical composition, molecular structure, extractives, and ash content.^{8–11} For example, in thermogravimetric analysis (TGA) experiments with low heating rates (<100°C/min), biomass materials decompose in well-described stages of moisture evolution, hemicellulose decomposition, and cellulose decomposition, whereas lignin is decomposed very slowly at a minor level.^{6,12} The decomposition mechanism of each component is also different. For example, cellulose chain length can be reduced by bond scission with the generation of free radicals involved in dehydration, the formation of carboxyl and carbonyl groups, CO₂ and CO emission, and carbon formation. Depolymerization of cellulose can also occur by scission of the glucosidic units and the formation of levoglucosan.⁶ The thermal degradation behavior of lignin is greatly influenced by complicated structures composed mainly of phenyl propane units.^{5,13,14} The thermal decomposition of hemicellulose also differs because of its various molecular structures. It has also been reported that high ash concentrations reduce hydrocarbon yields during thermochemical conversion.¹⁵

Correspondence to: S.-H. Lee (lshyhk@hotmail.com).

Seung-Hwan Lee shares the authorship with Hyun-Woo Cho.

The objective of this study was to predict thermal decomposition behavior with near infrared (NIR) spectroscopy and its multivariate analysis, which are known together as a rapid analysis tool for the characterization of biomass raw feedstock. To the best of our knowledge, there is as yet no direct approach that uses NIR spectroscopy to predict thermal decomposition behavior, although many studies have been done to characterize biomass quality in terms of chemical composition, extractives, ash and char content, and physical and anatomical properties.^{6,8,16,17} According to these studies, NIR, coupled with multivariate statistical techniques, has the capability to predict biomass properties. This study was conducted, on the basis of NIR spectroscopy and its multivariate analysis, to predict the weight-loss profile of biomass as a function of temperature in the expectation that this information would be meaningful to research on pyrolysis and gasification processes for bioenergy.

EXPERIMENTAL

Materials

Three woody biomass samples—red oak (*Quercus rubra*), yellow poplar (*Liriodendron tulipifera* L.), and hickory (*Carya alba*)—and three herbaceous biomass samples—switchgrass (*Panicum virgatum* L.), corn stover (*Zea mays* L.), and bagasse (*Saccharum* spp.)—were used for this study. Three different samples (18 samples total) were collected from each biomass. Wood samples were collected from different trees. The samples were ground to a 2-mm size by a Wiley cutter mill (Thomas Scientific, Swedesboro, NJ).

TGA measurements

A thermogravimetric analyzer (Pyris 1 TGA, Perkin Elmer, Shelton, CT) was used to investigate the weight-loss profiles of the biomass over the temperature range. Samples of 6–7 mg were first heated from 50 to 105°C at a rate of 25°C/min and kept at 105°C for 10 min to remove the moisture. Then samples were heated again to 750°C at the same heating rate within a nitrogen atmosphere (flow rate = 20 mL/min) to collect the thermograms.

NIR measurements

The NIR measurements were conducted with an Advanced Spectral Devices field spectrometer (ASD, Boulder, Co) at wavelengths between 500 and 2500 nm. A fiber-optic probe oriented at 60° to the sample surface was used to collect the reflectance spectra. A piece of commercial, microporous Teflon was used as the white reference material. The samples were illuminated with a high-intensity light at a right angle to

the sample surface. Three scans were collected from different location of samples. Three spectra collected on each sample (18 samples) were averaged to provide a single spectrum, which was used to predict the weight-loss profile from TGA measurement. We further reduced the data set by averaging the spectra that were collected at 1-nm intervals to a spectral data set at 10-nm intervals. Averaging the spectral data reduced the size of the spectra matrix and significantly reduced the time required to compute the partial least squares (PLS) prediction models without decreasing the quality of the models. The average spectra were used to perform a statistical analysis of the samples, which was implemented in MATLAB software (The MathWorks, Inc., Natick, MA).

PLS analysis

PLS is a multivariate projection method for modeling a relationship between independent variables (X values) and dependent variables (Y values). PLS seeks to find a set of latent variables that maximizes the covariance between X ($X = Mn$) and Y ($Y = MN$), where M represents the number of samples, n is the number of independent variables, and N stands for the number of dependent variables. It decomposes X and Y into the forms:

$$X = \mathbf{T}\mathbf{P}^T + \mathbf{E} \quad (1)$$

$$Y = \mathbf{U}\mathbf{Q}^T + \mathbf{F} \quad (2)$$

where \mathbf{T} and \mathbf{U} ($= MA$) are the matrices of the extracted A score vectors, \mathbf{P} ($= nA$) and \mathbf{Q} ($= MA$) are the loading matrices, and \mathbf{E} ($= Mn$) and \mathbf{F} ($= MN$) are the residual matrices. The PLS method searches for weight vectors (\mathbf{W} and \mathbf{C}) that maximize the sample covariance between \mathbf{t} and \mathbf{u} , where \mathbf{t} and \mathbf{u} are X -scores and Y -scores of a component, respectively (Wold, 1975). By regressing $X(Y)$ on $\mathbf{t}(\mathbf{u})$, the loading vector $\mathbf{p}(\mathbf{q})$ can be computed as follows:

$$\mathbf{p} = (\mathbf{t}^T\mathbf{t})^{-1}\mathbf{X}^T\mathbf{t} \quad (3)$$

$$\mathbf{q} = (\mathbf{u}^T\mathbf{u})^{-1}\mathbf{Y}^T\mathbf{u} \quad (4)$$

Then, the PLS regression model can be expressed as $Y = \mathbf{X}\mathbf{B} + \mathbf{G}$, where \mathbf{G} is the residual vector. Here B represents the regression coefficient, which is given by

$$B = \mathbf{W}(\mathbf{P}^T\mathbf{W})^{-1}\mathbf{C}^T = \mathbf{X}^T\mathbf{U}(\mathbf{T}^T\mathbf{X}\mathbf{X}^T\mathbf{U})^{-1}\mathbf{T}^T\mathbf{Y} \quad (5)$$

Orthogonal signal correction (OSC)

Before a prediction model was built for the NIR data and weight-loss profile with temperature, a

preprocessing method of OSC was applied to the original NIR data. OSC can selectively remove the largest variation of the predictor variable X that is orthogonal or unrelated to the response variable Y .¹⁸ This is possible because an OSC uses the response Y to construct a kind of signal filter for X . The main purpose of OSC-based preprocessing is to improve the predictive power of the prediction model by removing unwanted variations of the NIR data that do not contribute to prediction. Since the introduction of the OSC by Wold et al.,¹⁹ several OSC algorithms have been reported.^{19–21} Here, a direct OSC algorithm developed by Westerhuis et al.²¹ was used because of its high reliability. The PLS model constructed on the basis of the OSC-treated data of 54 samples was able to explain 92.9% of the Y variation (denoted as R^2Y). This model had a higher predictive power of 82.3% than that of 58.1% obtained from an original data-based PLS model ($R^2Y = 62.6\%$).

Wavelet

Wavelet transform provides a powerful signal analysis tool by transferring a mapping from a time domain to a time-scale domain. An original signal is decomposed into its contributions at different regions of a time-scale space. One performs this decomposition by projecting it onto corresponding wavelet basis functions. A wavelet is a family of functions derived from a basis function $[\psi(t)]$ defined in terms of two parameters, dilation (a ; scale) and translation (b ; time):

$$\Psi_{a,b}(t) = 2^{-a/2}\psi(2^{-a}t - b) \quad (6)$$

The wavelet is either stretched or compressed to create other scales, which change the width of the windows. This property makes a wavelet suitable to describe different features of the signal: wavelet coefficients at finer levels are used to capture sharp features, and wavelet coefficients at coarser levels are used to capture broad or smooth features. The wavelet coefficient can be obtained by the dot product between a signal $[f(t)]$ and a wavelet function:

$$\langle f(t), \Psi_{a,b}(t) \rangle = \int f(t)\Psi_{a,b}(t)dt \quad (7)$$

Denosing is achieved by the selection of wavelet coefficients that have valuable information. Many wavelet thresholding procedures have been developed on the basis of the idea of selecting important wavelet coefficients and setting unimportant ones to zero. For example, VisuShrink,²² SURE (Stein's unbiased estimate of the risk function),²³ and AMDL (approximate minimum description length)²⁴ procedures have been developed. However, most of the procedures involve only a single curve. The applica-

tion of single-curve-based procedures to multiple curves will lead to different selections of important wavelet coefficients in different curves. In this study, the vertical energy thresholding procedure developed by Jung et al.²⁵ was used to build a prediction model based on multiple NIR data.

Root-mean-square error (RMSE)

A cross-validation method based on the predicted residual error sum of squares was used in this study to select the number of latent variables for the PLS models.²⁶ In this study, we adopted as a measure of the predictive performance of a prediction model the RMSE values of residuals, which were defined as

$$\text{RMSE} = \sqrt{\frac{\sum_{i=1}^n (y_i - \hat{y}_i)^2}{n}} \quad (8)$$

where y_i is the true value, \hat{y}_i is the predicted value, and n is the total number of samples. PLS and wavelet analysis were performed with MATLAB software (The MathWorks, Inc., Natick, MA) and WaveLab v. 802, respectively.

RESULTS AND DISCUSSION

Figure 1 shows the weight-loss profile and derivative thermogravimetry (DTG) as a function of temperature for six lignocellulosic biomass samples (Biomass Technology Research Center, Hiroshima, Japan). The decomposition behavior differed in all samples. In particular, big differences occurred between woody biomass (red oak, yellow poplar, and hickory) and herbaceous biomass (corn stover, switchgrass, and bagasse), which showed that the woody biomass had a lower onset decomposition temperature in the thermograms and a lower main decomposition peak in the DTG curves than the herbaceous biomass. Furthermore, in the case of herbaceous biomass, three clear stages of decomposition were shown in the DTG curves. For example, switchgrass showed a first stage with a small hump in the temperature range from 180 to 220°C, which was characteristic of low-molecular-weight components, such as hemicellulose, and a second stage at higher temperatures in the range 250–300°C, which corresponded to the thermal degradation of cellulose. A third one near 340°C was due to lignin decomposition. On the other hand, the decomposition of woody biomass could largely be divided into the following steps: 220–315°C was predominantly hemicellulose decomposition, 315–380°C was cellulose decomposition, and 380°C and above was lignin decomposition. As mentioned in the Introduction, it is a well-known phenomenon in the research field of biomass pyrolysis and gasification that all these

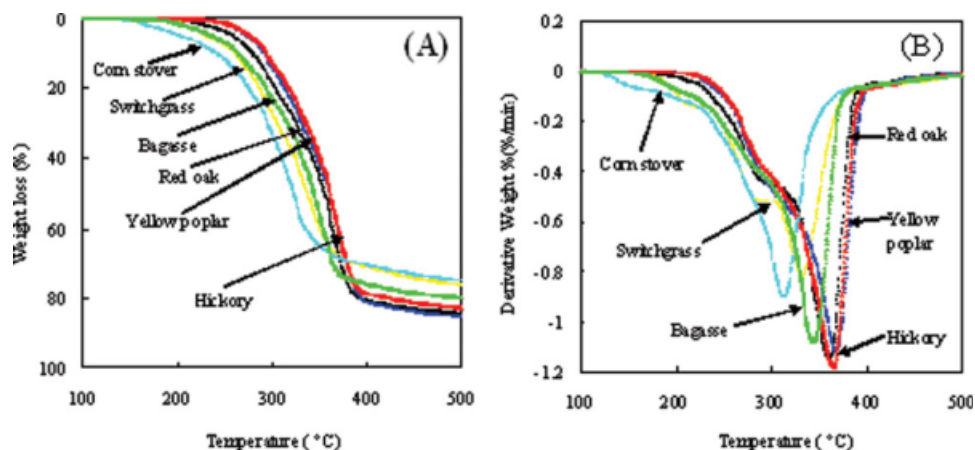


Figure 1 (A) Thermograms and (B) DTG curves of all biomass obtained by TGA measurements (heating rate = 25°C/min). [Color figure can be viewed in the online issue, which is available at www.interscience.wiley.com.]

differences are because of the differences in chemical composition, molecular weight and structure, extractives, ash content, and so on.^{8,27}

It was well illustrated in previous reports that NIR spectroscopy, combined with statistical analysis, is a very useful tool for characterizing biomass.^{6,8,16,17} Our interest stemmed from the fact that the NIR spectra of biomass include a lot of information, such as chemical composition and physical, mechanical, and structural properties, that affect the thermal decomposition behavior.

The prediction of a weight-loss profile of biomass over a range of temperatures was conducted by the analysis of the NIR spectra with a multivariate calibration model. The high dimensionality and collinearity in the NIR spectra data make it difficult in some cases to construct a prediction model.²⁸ This is attributed to the fact that in this study the number of samples (i.e., 54) is much smaller than the number of independent variables (i.e., 538). In addition, the NIR spectra data are obtained from digitized continuous signals so that the independent variables neighboring in the spectra are thus highly correlated. This can be solved by the adoption, before a model is built, of an effective compression tool based on a wavelet transform. This sequence works because NIR spectra are quite redundant by nature and thus suitable for compression. The NIR spectra data need to be compressed by the wavelet transform, followed by the perform-

ance regression analysis on some of the wavelet coefficients. For regression analysis purposes, a multivariate regression method of PLS can be used. PLS has proven to be useful in various regression problems.^{20,29,30} In particular, PLS has been shown to be a powerful technique for multivariate calibration of noisy, collinear, high-dimensional, and ill-conditioned data.²⁸

To evaluate the performance of the proposed prediction model with test data, a leave-3-out procedure was performed on the 54 NIR spectra because 3 samples in the same type of biomass showed similar temperature profiles. That is, 3 of the 54 spectra were kept out of the prediction model development, and these were then predicted by the prediction model. Then, this procedure was repeated several times until every sample had been kept out once and only once. Such a leave-3-out test procedure is used to evaluate the prediction model through the use of samples that are not included in the model-building stage. Thus, this procedure may indicate how reliable the prediction model would be in practice when unknown samples are predicted. A critical parameter that determines the performance of PLS models is the number of latent variables retained. This number should be determined by consideration of both the curse of dimensionality and the loss of data information. In this study, a measure of the predicted residual error sum of squares was used to select the number of optimal latent variables.

TABLE I
Results of RMSEP and Adjusted R^2 Values for 10 Temperature Points: Ordinary PLS Versus Wavelet PLS

		Temperature									
		150°C	200°C	250°C	300°C	350°C	400°C	450°C	500°C	550°C	600°C
Ordinary PLS	RMSEP	0.1423	0.7416	1.1756	3.5449	6.7114	4.3479	4.0251	3.7626	3.9069	4.2767
	Adjusted R^2	0.974	0.963	0.957	0.909	0.828	0.832	0.845	0.840	0.808	0.793
Wavelet PLS	RMSEP	0.1025	0.5953	1.1941	2.7396	5.2447	1.8118	1.7103	2.0316	2.8508	3.6569
	Adjusted R^2	0.981	0.976	0.955	0.913	0.852	0.887	0.891	0.880	0.843	0.827

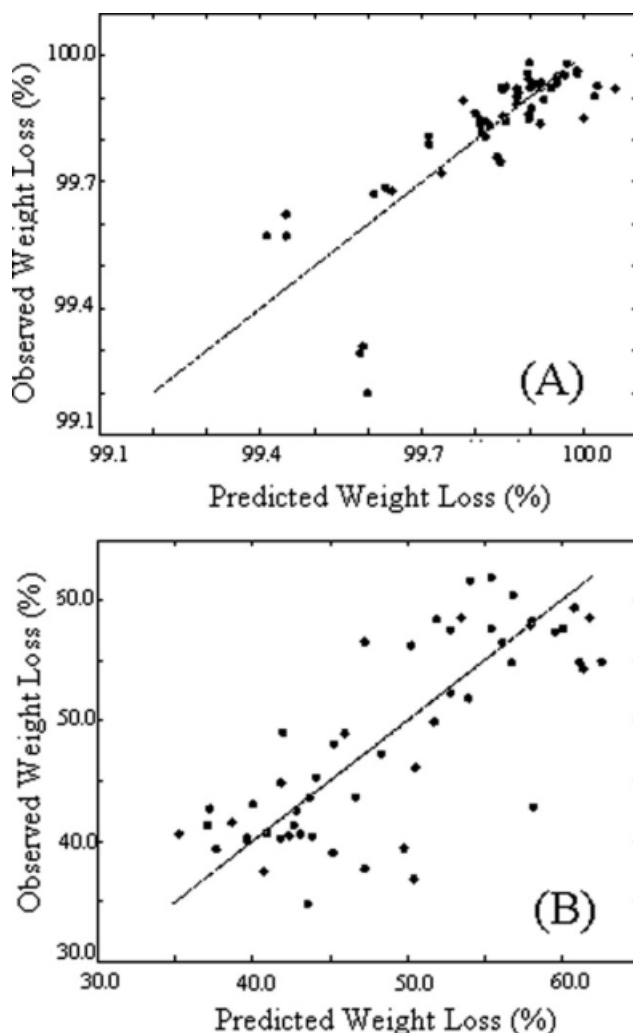


Figure 2 Plots of observed and predicted weight losses (%) at (A) 150 and (B) 350°C with wavelet PLS.

Table I shows the prediction results of the RMSE values [i.e., the root-mean-square error in prediction (RMSEP) values] and adjusted R^2 values for the

selected 10 temperature points (i.e., 150, 200, 250, 300, 350, 400, 450, 500, 550, and 600°C). For comparison purposes, two PLS prediction models, which were based on ordinary PLS and OSC-treated wavelet PLS, were built and evaluated. In the wavelet PLS, the vertical energy thresholding method selected only 49 wavelet coefficients. In this study, a Symmlet-8 wavelet was used to build the wavelet PLS prediction model. As shown in Table I, the wavelet PLS model produced lower RMSE values for all response variables of the 10 temperature points; thus, it showed a significantly better predictive performance than the ordinary PLS model.

The proposed prediction model, for example, was able to predict the weight loss percentage at 150°C with $RMSEP = 0.1025$, whereas the ordinary PLS predicted it with $RMSEP = 0.1423$. In both PLS models, the response for the weight loss at 150°C showed a minimum RMSEP value and a maximum RMSEP value for the weight loss at 350°C. This means that the response values of weight loss at 150°C were predicted more successfully than those at 350°C. The proposed prediction model, for example, was able to predict the weight loss percentage at 150°C with $RMSEP = 0.1025$, whereas the ordinary PLS predicted it with $RMSEP = 0.1423$. In both PLS models, the response for the weight loss at 150°C showed a maximum R^2 value of 97.4%, although there were some underestimated observations, as shown in Figure 2(A), and a minimum R^2 value of 82.80% for the weight loss at 600°C. As shown in Figure 2, the predictions of the weight loss at 350°C showed larger variations than that at 150°C.

To visualize the predictive performance of the proposed prediction model, the predicted weight loss profiles were plotted against those observed with temperature, as shown in Figure 3 [yellow poplar in Fig. 3(A) and switchgrass in Fig. 3(B)]. As expected, low RMSE values resulted in little

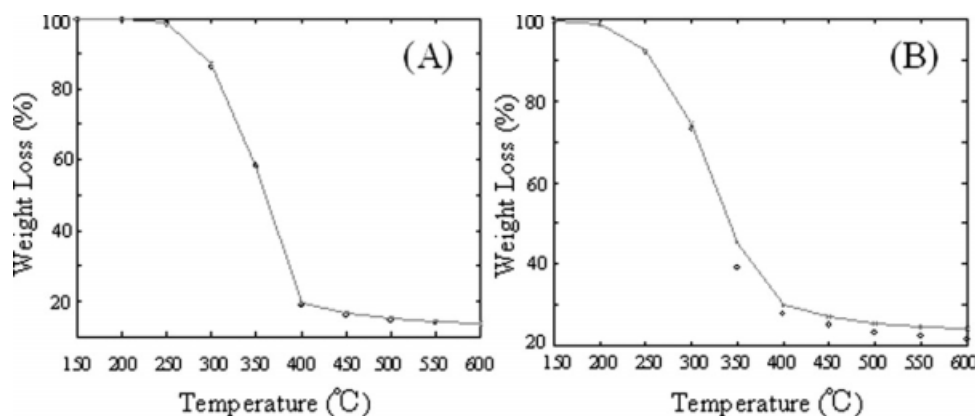


Figure 3 Weight-loss profiles with temperature corresponding to (A) a sample of yellow poplar and (B) a sample of switchgrass. Circles indicate the observed values, and the crossed lines show the predicted values.

deviation between the predicted and observed response variables. Such a good performance of the wavelet PLS prediction model can be explained by a comparison of the original and reconstructed data. Only 49 wavelet coefficients out of 538 were used to reconstruct the original curves, and the reconstruction results were quite successful. In this case, only 9.11% of the original information was good enough to capture the important patterns of the NIR data needed to build a prediction model.

CONCLUSIONS

The NIR spectra of three types of woody biomass and three types of herbaceous biomass were successfully analyzed to predict their thermal decomposition behavior. The weight losses at 10 temperatures measured by TGA measurement were well matched with the ones obtained by the wavelet PLS model, which showed better predictive performance than the ordinary PLS model. This study showed the possibility of using NIR spectra to characterize the thermal decomposition behavior of lignocellulosic biomass for energy production. However, more accurate prediction and a field-acceptable calibration model will require more diverse samples from different origins and more in-depth TGA experiments with different measurement conditions, such as isothermal measurements, different environments, and other related parameters.

References

1. Yang, B.; Wyman, C. E. *Biotechnol Bioeng* 2006, 94, 611.
2. Pan, X. J.; Gilkes, N.; Kadla, J.; Pye, K.; Saka, S.; Gregg, D.; Ehara, K.; Xie, D.; Lam, D.; Saddler, J. *Biotechnol Bioeng* 2006, 94, 851.
3. Lin, Y.; Tanaka, S. *Appl Microbiol Biotechnol* 2006, 69, 627.
4. Yang, H. P.; Yan, R.; Chen, H. P.; Zheng, C. G.; Lee, D. H.; Liang, D. T. *Combust Flame* 2006, 146, 605.
5. Butt, D. A. E. *J Anal Appl Pyrolysis* 2006, 76, 38.
6. Sanderson, M. A.; Agblevor, F.; Collins, M.; Johns, D. K. *Biomass Bioenergy* 1996, 11, 361.
7. Trebbi, G. *Bioresour Technol* 1993, 46, 23.
8. Kelley, S. S.; Rials, T. G.; Snell, R.; Groom, L. H.; Sluiter, A. *Wood Sci Technol* 2004, 38, 257.
9. Fisher, T.; Hajaligol, M.; Waymack, B.; Kellogg, D. *J Anal Appl Pyrolysis* 2002, 62, 331.
10. Torbjörn, A.; Rhén, L. C. *Analyst* 2005, 130, 1182.
11. Stenseng, M.; Jensen, A.; Johansen, K. D. *J Anal Appl Pyrolysis* 2001, 58, 765.
12. Clark, D. H.; Mayland, H. F.; Lamb, R. C. *Agronomy J* 1987, 79, 485.
13. Li, J.; Li, B.; Zhang, X. *Polym Degrad Stab* 2002, 78, 279.
14. Ramiah, M. V. *J Appl Polym Sci* 1970, 14, 1323.
15. Agblevor, F. A.; Rejai, B.; Evans, R. J.; Johnson, K. D. *Energy from Biomass and Wastes XVI*; Elsevier Applied Science: Chicago, 1992; p 767.
16. Pizarro, C.; Esteban-Diez, I.; Nistal, A. J.; González-Sáiz, J. M. *Anal Chim Acta* 2004, 509, 217.
17. Woo, Y. A.; Kim, H. J.; Park, S. Y.; Chang, S. Y.; Chung, H. *Microchem J* 1999, 63, 154.
18. Wold, S.; Antti, H.; Lindgren, F.; Öhman, J. *Chemom Intell Lab Syst* 1998, 44, 175.
19. Sjöblom, J.; Svensson, O.; Josefson, M.; Kullberg, H.; Wold, S. *Chemom Intell Lab Syst* 1998, 44, 229.
20. Fearn, T. *Chemom Intell Lab Syst* 2000, 50, 47.
21. Westerhuis, J. A.; Jong, S.; Smilde, A. K. *Chemom Intell Lab Syst* 2001, 56, 13.
22. Donoho, D. L.; Johnstone, I. M. *Biometrika* 1994, 81, 425.
23. Donoho, D. L.; Johnstone, I. M. *Biometrika* 1995, 81, 425.
24. Saito, N. *Wavelets in Geophysics*; Academic: New York, 1994; p 299.
25. Jung, U.; Jeong, M.; Lu, J. C. *IEEE Trans Syst Man Cybernet B* 2006, 36, 1128.
26. Barker, M.; Rayens, W. *J Chemom* 2003, 17, 166.
27. Skodras, G.; Grammelis, P.; Basinas, P.; Kakaras, E.; Sakellariopoulos, G. *Ind Eng Chem Res* 2006, 45, 3791.
28. Qin, S. J. *J Chemom* 2003, 17, 480.
29. Kourtji, T. *Int J Adapt Control Signal Process* 2005, 19, 213.
30. Rosipal, R.; Trejo, L. J. *J Machine Learn Res* 2001, 2, 97.